lubricants

MDPI

Article

Friction and Wear Characteristics of Aqueous ZrO_2/GO Hybrid Nanolubricants

Shuiquan Huang [1,2], Zhen Wang [1], Longhua Xu [1] and Chuanzhen Huang [1,*]

[1] School of Mechanical Engineering, Yanshan University, Qinhuangdao 066004, China; shuiquan.huang@ysu.edu.cn (S.H.); wangzhen@ysu.edu.cn (Z.W.); longhua1357@ysu.edu.cn (L.X.)
[2] School of Mechanical and Mining Engineering, The University of Queensland, Brisbane 4072, Australia
* Correspondence: huangchuanzhen@ysu.edu.cn

Abstract: Aqueous nanolubricants containing ZrO_2 nanoparticles, graphene oxide (GO) nanosheets, or hybrid nanoparticles of ZrO_2 and GO were formulated using a cost-effective ultrasonication de-agglomeration method. The friction and wear characteristics of these water-based nanolubricants were systematically investigated using a block-on-ring testing configuration with a stainless- and alloy steel contact pair. The concentrations and mass ratios of nanoadditives were varied from 0.02 to 0.10 wt.% and 1:5 to 5:1, respectively, to obtain optimal lubrication performance. The application of a 0.06 wt.% 1:1 ZrO_2/GO hybrid nanolubricant resulted in a 57% reduction in COF and a 77% decrease in wear volume compared to water. The optimised ZrO_2/GO hybrid nanolubricant was found to perform better than pure ZrO_2 and GO nanolubricant in terms of tribological performance due to its synergistic lubrication effect, which showed up to 54% and 41% reductions in friction as well as 42% and 20% decreases in wear compared with 0.06 wt.% ZrO_2 and 0.06 wt.% GO nanolubricants. The analysis of wear scars revealed that using such a ZrO_2/GO hybrid nanolubricant yielded a smooth worn surface, with 87%, 45%, and 33% reductions in S_a compared to water and 0.06 wt.% ZrO_2 and 0.06 wt.% GO nanolubricants. The superior tribological performance can be ascribed to the combination of the rolling effect of ZrO_2 nanoparticles and the slipping effect of GO nanosheets.

Keywords: water-based nanolubricant; zirconia; graphene oxide; hybrid nanoparticles; friction; wear

Citation: Huang, S.; Wang, Z.; Xu, L.; Huang, C. Friction and Wear Characteristics of Aqueous ZrO_2/GO Hybrid Nanolubricants. *Lubricants* **2022**, *10*, 109. https://doi.org/10.3390/lubricants10060109

Received: 12 May 2022
Accepted: 31 May 2022
Published: 1 June 2022

1. Introduction

Mineral-oil-based lubricants are commonly used for industrial lubrication; however, their usage is frequently seen to raise environmental, health, and economic concerns due to their non-biodegradable nature and inherent toxicity [1–5]. In this context, water-based lubricants have recently attracted increasing academic and industrial interest, because they are clean and environmentally friendly [6–11]. However, water alone cannot offer satisfactory lubrication because of its low lubricity and weak load-carrying capability. High-performance additives are therefore introduced into water-based lubricants for enhancing their friction-reduction and anti-wear capacities.

Innovative nanoparticles with a near-spherical/rounded shape and a high load-carrying capacity including SiO_2, Al_2O_3, and ZrO_2 [12–16], carbon-based nanosheets of low shear resistance such as graphene and graphene oxide (GO) [17–20], and clay nanomaterials of low cost such as montmorillonite and zeolite [21–23] have recently been applied to water-based lubrication for achieving improved tribological and machining performance [24–27]. For example, zero-dimensional (0D) Al_2O_3 nanoparticles of 30 nm were added to water to prepare an Al_2O_3 nanolubricant for alloy steel on stainless steel contact [15]. The nanolubricant formed a dynamically balanced tribo-layer during sliding, improving surface asperity contact, and thus lowered friction and wear by 27% and 22% compared with a water lubricant. The friction and wear of an alloy steel ball sliding against a low-carbon microalloyed steel disk was considerably reduced when using a water-based TiO_2 nanolubricant of 20 nm, because of its mending and rolling effects [28]. Two-dimensional graphene

nanosheets were dispersed in water for chromium steel on carbon steel contact, which resulted in respective 53% and 91% reductions in friction and wear rate compared with water attributed to graphene's slipping effect [29]. An aqueous nanolubricant containing GO nanosheets of 2 nm thickness was found to produce a self-lubricating film to mitigate asperity ploughing during sliding, thus lowering the contact friction of an alloy steel ball on stainless-steel plate by around 45% in comparison to deionised water [30]. Due to their satisfactory tribological performance, water-based nanolubricants have recently been applied to different processes, such as rolling [31], turning [32], milling [21], and grinding [25], for achieving high-performance and green manufacturing. For example, a 4.0 wt.% TiO_2 nanolubricant was innovatively used to hot roll low-carbon microalloyed steels, which performed comparably to a conventional 1.0 vol.% oil-in-water lubricant in terms of rolled strip surface quality and rolling forces at rolling temperatures of 850 and 950 ∘C [31]. Water-based nanolubricants containing CuO, ZnO, Fe_2O_3, or Al_2O_3 were also developed for turning AISI 4340 steels [32]. The CuO nanolubricant presented a great heat-carrying capacity, and it produced a protective film that resulted in a decreased cutting force and reduced tool wear. Water-based GO nanolubricants were employed for grinding GaAs wafers [24] and GGG laser crystals [25], which significantly reduced friction at the abrasives–workpiece interface, resulting in a much lower grinding force and improved surface quality compared with an emulsion coolant. In recent years, due to their excellent tribological performance and low-cost and environment-friendly nature, a water-based lubricant using montmorillonite clay nanoparticles as additives were employed to mill AISI 1018 steel plates [22] and AISI 4340 steel bars [33]. The nanolubricant performed better than a conventional mineral-oil-based emulsion in terms of machined surface quality and tool life. Although much work has shown promising tribological and machining results when using 0D or 2D nanomaterials as lubricant additives, these nanoadditives in water lubricants have a tendency to agglomerate or restack due to their high surface energy and activity. This causes sedimentation, increasing particle size, and limits formation of self-lubricating films, thus resulting in failure of lubrication [34].

In recent years, the use of hybrid nanoparticles as lubricant additives, such as Al_2O_3/MoS_2 [35], TiO_2/GO [16], and TiO_2/montmorillonite clay [33], has been reported to be an effective approach to achieve improved lubrication performance. For instance, Huang et al. [34] synthesised an aqueous hybrid nanolubricant through dispersing Al_2O_3 nanoparticles in a water-based GO nanosheet solution, and found that such dimensional integration could relieve Al_2O_3 agglomeration and restrain GO restacking in water. The Al_2O_3/GO nanolubricant thus produced a significant decrease in friction and wear, as well as a considerable improvement in the worn surface quality compared to the nanolubricant only containing Al_2O_3 or GO nanoadditives. In addition to their environment-friendly and low-cost nature, ZrO_2 nanoparticles have demonstrated excellent desirable properties for water-based lubrication, such as high load-carrying capacity and excellent durability [16]. Hydrophilic GO nanosheets can form a stable suspension in water [19,30], which makes them attractive additives for water-based lubricants. However, until now, few efforts have been made to explore the tribological characteristics and mechanisms of water-based lubricants with ZrO_2/GO hybrid nanoparticles as additives [16].

In this work, aqueous hybrid nanolubricants were formulated by ultrasonically mixing ZrO_2 nanoparticles in GO suspensions. The tribological properties of the developed nanolubricants were systematically investigated utilizing a block-on-ring testing approach with stainless steel on alloy steel contact, with water serving as a benchmark lubricant. The concentrations and mass ratios of nanoadditives were changed to gain an optimal lubrication performance. The roles of nanoadditives in water-based lubrication were investigated and discussed.

2. Materials and Methods

2.1. Formulation of Nanolubricants

Zero-dimensional-ZrO_2 nanoparticles of ~30 nm in diameter (purchased from XF-NANO Co. Ltd., Nanjing, China) and 2D-GO nanosheets (supplied by Hengqiu Graphene Technology Co. Ltd., Suzhou, China) were used as nanoadditives. The GO nanosheets had a lateral diameter of ~5 µm and a thickness of 1~2 nm. Distilled water was employed as a base solvent. ZrO_2/GO hybrid nanolubricants were synthesised as follows. ZrO_2 nanoparticles and GO nanosheets were mechanically mixed in water at mass ratios of ZrO_2 to GO of 1:5, 2:4, 3:3, 4:2, and 5:1 with a fixed additive content of 0.06 wt.% [30]. The ZrO_2 and GO mixture suspensions were then processed using a 450 W high-intensity ultrasonic probe for 30 min to dimensionally integrate ZrO_2 with GO. The ZrO_2/GO nanolubricants with different contents of 0.02, 0.04, 0.06, 0.08, and 0.10 wt.% at a constant ZrO_2 to GO mass ratio of 1:1 were also formulated to optimise lubrication performance [34]. A ZrO_2 or GO nanolubricant with a 0.06 wt.% additive content was prepared for comparison.

The morphologies of ZrO_2 nanoparticles, GO nanosheets, and ZrO_2/GO hybrid nanoparticles dispersing in water were examined using transmission electron microscopy (TEM, JEM-2100, JEOL, Japan). In Figure 1a, ZrO_2 nanoparticles have a uniform size distribution with near-spherical/rounded shapes, but they are agglomerated in water, forming network clusters. The TEM image in Figure 1b shows that GO nanosheets are super-thin with micro-scale wide coverage, and are highly transparent with wrinkles on their surfaces. Figure 1c demonstrates that ZrO_2 nanoparticles are sparsely deposited onto GO nanosheets. The agglomeration sizes of ZrO_2 nanoparticles are much smaller than those shown in Figure 1a, indicating a better dispersion performance with dimensional hybridization of 0D nanoparticles and 2D nanosheets.

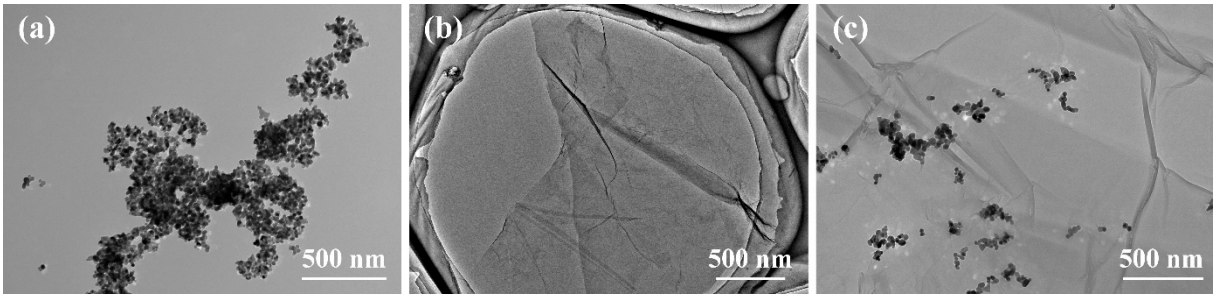

Figure 1. TEM images showing (**a**) GO nanosheets, (**b**) ZrO_2 nanoparticles, and (**c**) ZrO_2/GO hybrid nanoparticles dispersed in water.

2.2. Tribological Tests

The friction and wear performance of the formulated nanolubricants was assessed using a block-on-ring contact pair on a multi-specimen tribometer (UMT-3, Bruker, USA) [16]. Water was utilised as a benchmark lubricant for comparison. The block used was made of AISI 304 stainless steel and was ground with SiC abrasive paper of 15.3 µm before each test. The ring employed was made of AISI 52100 Cr alloy steel and was processed using a 15.3 µm SiC abrasive paper to maintain its surface texture. Considering the potential application in metal forming processes, the testing was performed at normal loads of 15, 20, 25, and 30 N, and sliding speeds of 200, 300, 400, and 500 mm/s with a fixed sliding distance of 12 m [5,31]. Each test was repeated three times, and average values were reported.

The steel blocks were ultrasonically cleaned in an acetone bath for 5 min after friction testing. The wear scar widths of the blocks were measured using a laser confocal microscope (LEXT OLS4100, Olympus, Tokyo, Japan). The wear volume (Vw, in mm^3) was then calculated using [23]:

$$V_w = \frac{D^2 t}{8}\left[2\sin^{-1}\frac{b}{D} - \sin\left(2\sin^{-1}\frac{b}{D}\right)\right] \quad (1)$$

where D is the diameter of the ring (35 mm), t is the width of the block (6 mm), and b is the average width of the wear scar. A scanning electron microscope (SEM, JEOL, JSM-6610, Tokyo, Japan) equipped with an energy-dispersive X-ray spectroscope (EDS) module and an inVia confocal Raman microscope (Renishaw plc., London, UK) was used to analyse the worn surfaces of the blocks.

3. Results and Discussion

3.1. Friction and Wear Properties of Nanolubricants

Figure 2 displays the coefficient of friction (COF) curves achieved from the tribological tests using water, 0.06 wt.% ZrO_2, 0.06 wt.% GO, and 0.03–0.03 wt.% ZrO_2/GO nanolubricants with a normal force of 20 N and a sliding speed of 300 mm/s. For all four tested lubricants, the COF reaches a steady state after running in for approximately 3 m. Water has a high COF of over 0.5 in the steady wear state. The addition of nanoadditives in water yields smaller COF values; particularly, the ZrO_2/GO nanolubricant produces the lowest COF value of approximately 0.23 among all the three tested nanolubricants, as shown in Figure 2. This result clearly indicates that the application of the hybrid nanolubricant produced the best interfacial lubrication.

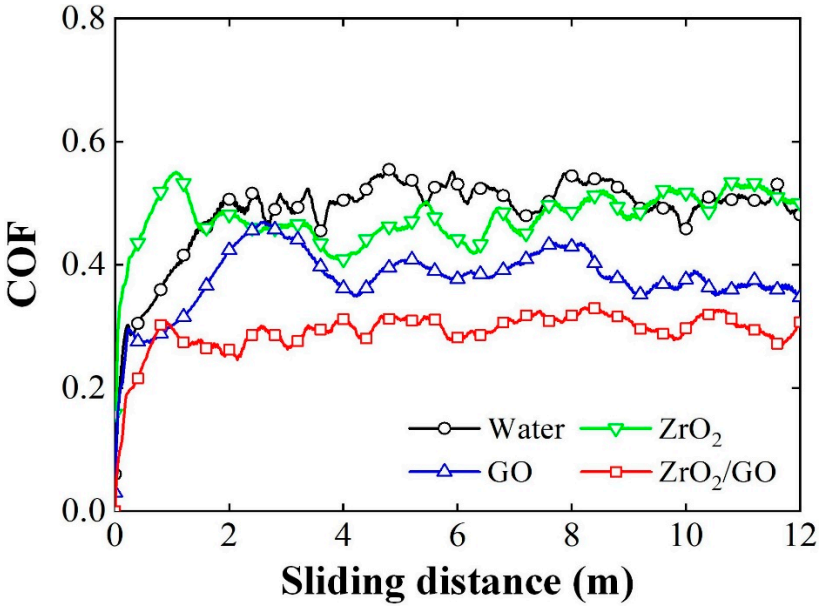

Figure 2. COF time histories generated using water, 0.06 wt.% ZrO_2, 0.06 wt.% GO, and 0.03–0.03 wt.% ZrO_2/GO nanolubricants. The friction tests were conducted at a normal force of 20 N and a sliding speed of 300 mm/s.

The effects of the mass ratio of ZrO_2 to GO and nanoadditive content on the averaged COF using ZrO_2/GO hybrid nanolubricants are shown in Figure 3. Note that the ZrO_2/GO content was fixed at 0.06 wt.%, and the COF values of water, the 0.06 wt.% ZrO_2, and 0.06 wt.% GO nanolubricants were plotted in the figure for comparison. It can be seen in Figure 3a that the addition of ZrO_2 or GO in water generates a lower COF value, indicating an improved interfacial lubrication performance. When ZrO_2/GO hybrid nanolubricants were employed, the COF decreased slightly and then increased significantly as the ZrO_2 to GO mass ratio changed from 1:5 to 5:1. The hybrid nanolubricant containing 0.03 wt.% ZrO_2 and 0.03 wt.% GO yielded the lowest COF, with its values being 57%, 54%, and 41% lower than those of the baseline water and the ZrO_2 and GO nanolubricants, respectively. The results suggest that such dimensional integration indeed helped improve the anti-friction performance of each nanoadditive. In other words, a synergistic lubricating action is in effect when using ZrO_2/GO nanocomposites as an additive in water [33,34].

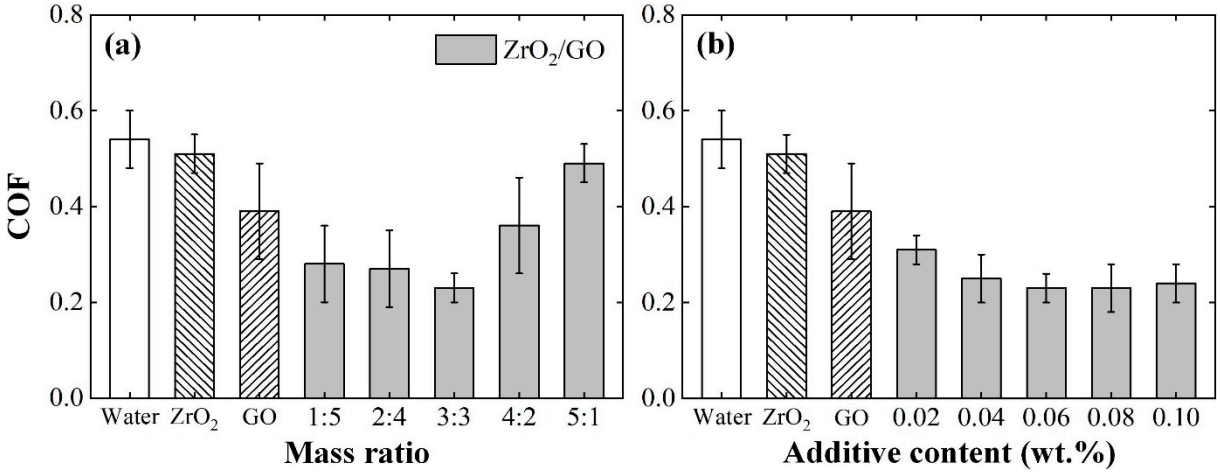

Figure 3. Effects of (**a**) ZrO_2 to GO mass ratio and (**b**) nanoadditive content on averaged COF with ZrO_2/GO nanolubricants at a testing load of 20 N and a sliding speed of 300 mm/s. The COF values of water and 0.06 wt.% ZrO_2 and 0.06 wt.% GO nanolubricants were used for comparison.

Figure 3b shows that the nanolubricants generate lower COF values than water, clearly confirming their good friction-reduction performance. When ZrO_2/GO nanolubricants were used, the increase in additive content from 0.02 to 0.06 wt.% resulted in a substantial decrease in COF, and a further increase in content had an insignificant effect on the COF. This result indicates that nanoadditive content indeed has an optimal value regarding lubrication performance, as reported in He et al. [15]. Again, the ZrO_2/GO hybrid nanolubricant produces lower interfacial friction compared to the ZrO_2 and GO nanolubricants for all the tested contents, as illustrated in Figure 3b, which was most likely due to its synergistic lubrication effect.

Figure 4 shows the effects of nanoadditive mass ratio and content on the averaged wear volume (WV) produced using the ZrO_2/GO hybrid nanolubricants at a normal load of 20 N and a sliding speed of 300 mm/s. Similarly, the WV values of water and the 0.06 wt.% ZrO_2 and 0.06 wt.% GO nanolubricants were included in the figure for comparison. The ZrO_2 and GO nanolubricants generated significantly less wear than water, with a higher WV value for the ZrO_2 nanolubricant due to the polishing effect of the ZrO_2 nanoparticles [7]. As shown in Figure 4a, for the ZrO_2/GO nanolubricants the effect of mass ratio on the wear loss is inconsistent. The hybrid nanolubricant with a ZrO_2-GO mass ratio of 3 to 3 generates the smallest wear volume, showing up to 42% and 20% reductions compared with the ZrO_2 and GO nanolubricants. A further increase in the mass percentage of ZrO_2 nanoparticles causes a substantial increase in wear attributed to the increased polishing effect as more ZrO_2 nanoparticles are involved in sliding.

Figure 4b depicts that the GO-related nanolubricants produce smaller wear volume values than the baseline water and the ZrO_2 nanolubricant. This is likely because 2D-GO nanosheets have better lubricity than 0D nanoparticles in water-based lubrication [36]. The wear loss of the ZrO_2/GO hybrid nanolubricants is significantly less than that of water at all the tested contents, as displayed in Figure 4b, indicating improved wear resistance. Again, the hybrid nanolubricant containing 0.03 wt.% ZrO_2 and 0.03 wt.% GO yielded the least wear.

The friction and wear results clearly indicate that aqueous nanolubricants with ZrO_2/GO hybrid nanoadditives could produce a synergistic lubrication effect in friction and wear reduction. The nanoadditive mass ratio and content indeed had optimal values in terms of friction-reduction and anti-wear performance. The ZrO_2/GO nanolubricant of a ZrO_2 to GO mass ratio of 1:1 with a content of 0.06 wt.% was thus selected for further tests.

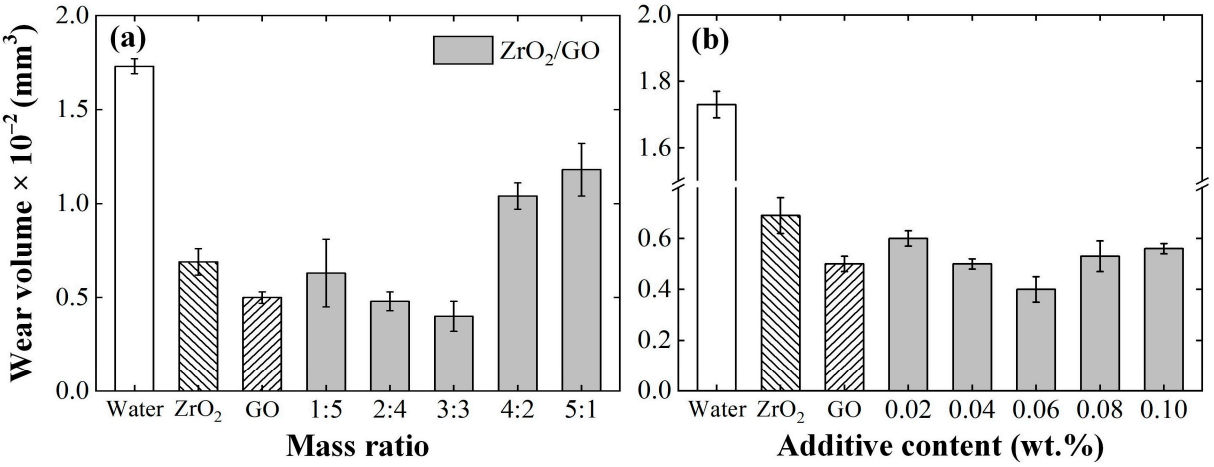

Figure 4. Effects of (**a**) ZrO_2 to GO mass ratio and (**b**) nanoadditive content on averaged wear volume using ZrO_2/GO nanolubricants. The wear volume values of water and 0.06 wt.% ZrO_2 and 0.06 wt.% GO nanolubricants were used for comparison. Applied load = 20 N and sliding speed = 300 mm/s.

3.2. Effect of Testing Conditions on Friction-Reduction Performance

The COF values of the 0.06 wt.% ZrO_2, 0.06 wt.% GO, and 0.03–0.03 wt.% ZrO_2/GO nanolubricants are plotted in Figure 5, as a function of applied load or sliding speed. The results achieved with water were used as benchmarks. In Figure 5a, a higher load yields a higher COF for all four tested lubricants as a result of the increased pressure of contact. However, the ZrO_2/GO hybrid nanolubricant produced the smallest COF compared to those obtained using water and the ZrO_2 and GO nanolubricants, clearly demonstrating its better performance in reducing friction. It can be seen from Figure 5b that the COF decreases with the increase in sliding speed for all the tested lubricants because of the reduced ploughing intensity of surface asperities. The ZrO_2 nanolubricant generated slightly smaller COF in comparison to water at all the tested speeds. The ZrO_2/GO hybrid nanolubricant, however, resulted in the lowest COF, followed by the GO nanolubricant.

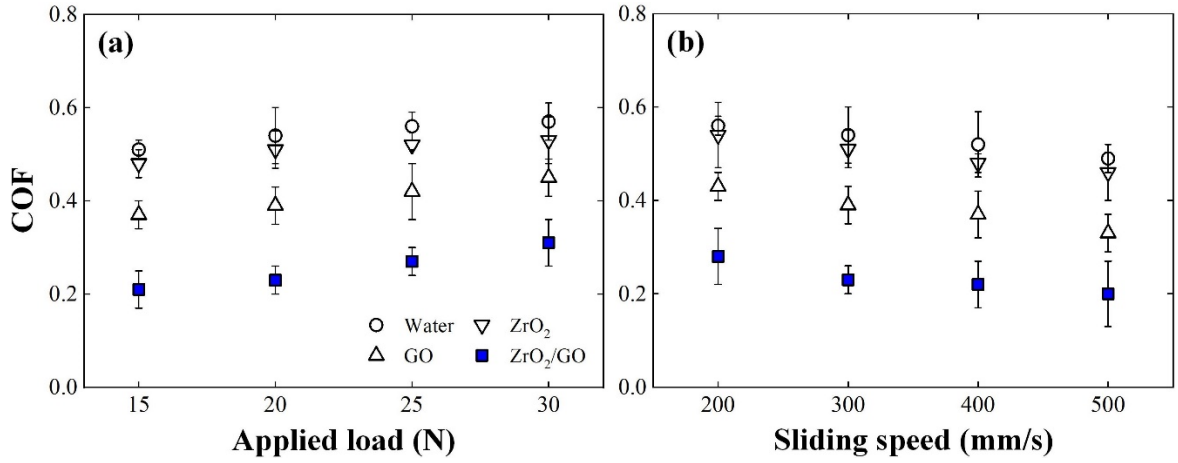

Figure 5. Effects of (**a**) applied load and (**b**) sliding speed on COF produced using water and 0.06 wt.% ZrO_2, 0.06 wt.% GO, and 0.03–0.03 wt.% ZrO_2/GO nanolubricants.

3.3. Effect of Testing Conditions on Anti-Wear Performance

Figure 6 displays the effects of testing load and speed on the wear volume produced using water and the ZrO_2, GO, and ZrO_2/GO nanolubricants. For all four tested lubricants, the wear volume increases substantially with the increase in applied load from 15 to 30 N. This is because a higher load could increase the ploughing intensity of surface asperities of the ring, thus resulting in the higher material removal of the block. The ZrO_2/GO

hybrid nanolubricant yields the lowest wear volume, as shown in Figure 6a, indicating the significantly improved asperity contact with the hybrid nanoadditives. In Figure 6b, a faster sliding speed generates less wear for all the tested lubricants, with the smallest wear volume achieved by the ZrO_2/GO hybrid nanolubricant. The results again demonstrate the effectiveness of the hybrid nanoparticles in improving the wear resistance of water.

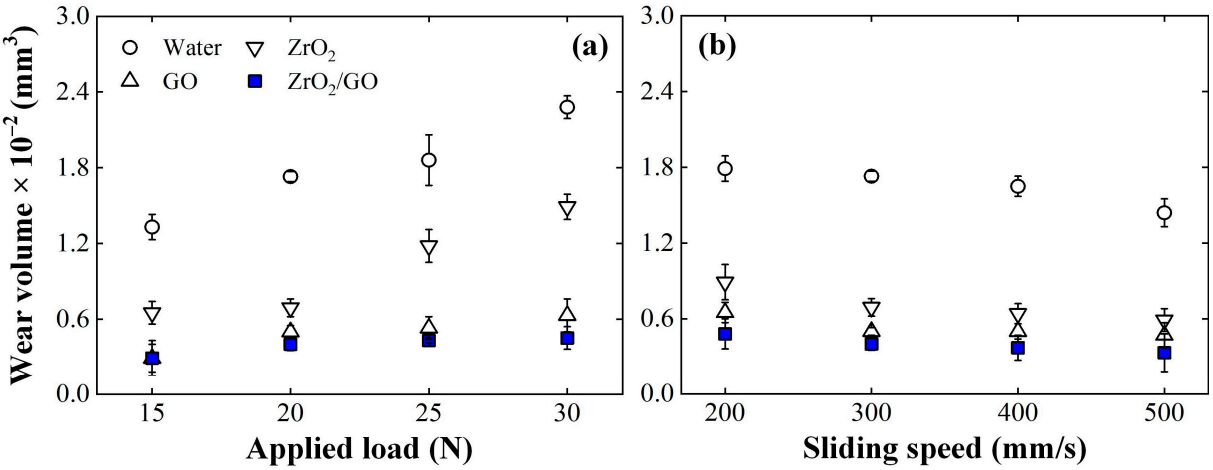

Figure 6. Effects of (**a**) applied load and (**b**) sliding speed on wear volume produced using water and 0.06 wt.% ZrO_2, 0.06 wt.% GO, and 0.03–0.03 wt.% ZrO_2/GO nanolubricants.

3.4. Worn Surface Characteristics

Figure 7 presents the SEM micrographs of the worn surfaces lubricated with water and the 0.06 wt.% ZrO_2, 0.06 wt.% GO, and 0.03–0.03 wt.% ZrO_2/GO nanolubricants at a normal force of 20 N and a sliding speed of 300 mm/s. In Figure 7a, delamination with slight grooves is clearly observed on the worn surface produced with water. During sliding, water had a weak capacity to relieve the "cold welding" of surface asperities due to its poor lubricity, thus resulting in the occurrence of material adhesion and peeling (see Figure 7b). The addition of ZrO_2 or GO improved asperity contact, thus producing a smoother surface with more visible ploughing grooves in comparison with water, as displayed in Figure 7b,c. The corresponding enlarged images shown in Figure 7f,g demonstrate that the sliding with the ZrO_2 and GO nanolubricants is mainly in the abrasive wear regime. It can be seen in Figure 7d,h that the ZrO_2/GO nanolubricant yields the smoothest worn surface and has no delamination in the sliding area due to its excellent synergistic lubrication performance. The performance of the ZrO_2/GO nanolubricant in surface quality improvement was also quantitatively compared with water and the ZrO_2 and GO lubricants. As depicted in Figure 8, the ZrO_2/GO nanolubricant produces the lowest surface roughness, with 87%, 45%, and 33% reductions in S_a compared to water and the ZrO_2 and GO nanolubricants, respectively.

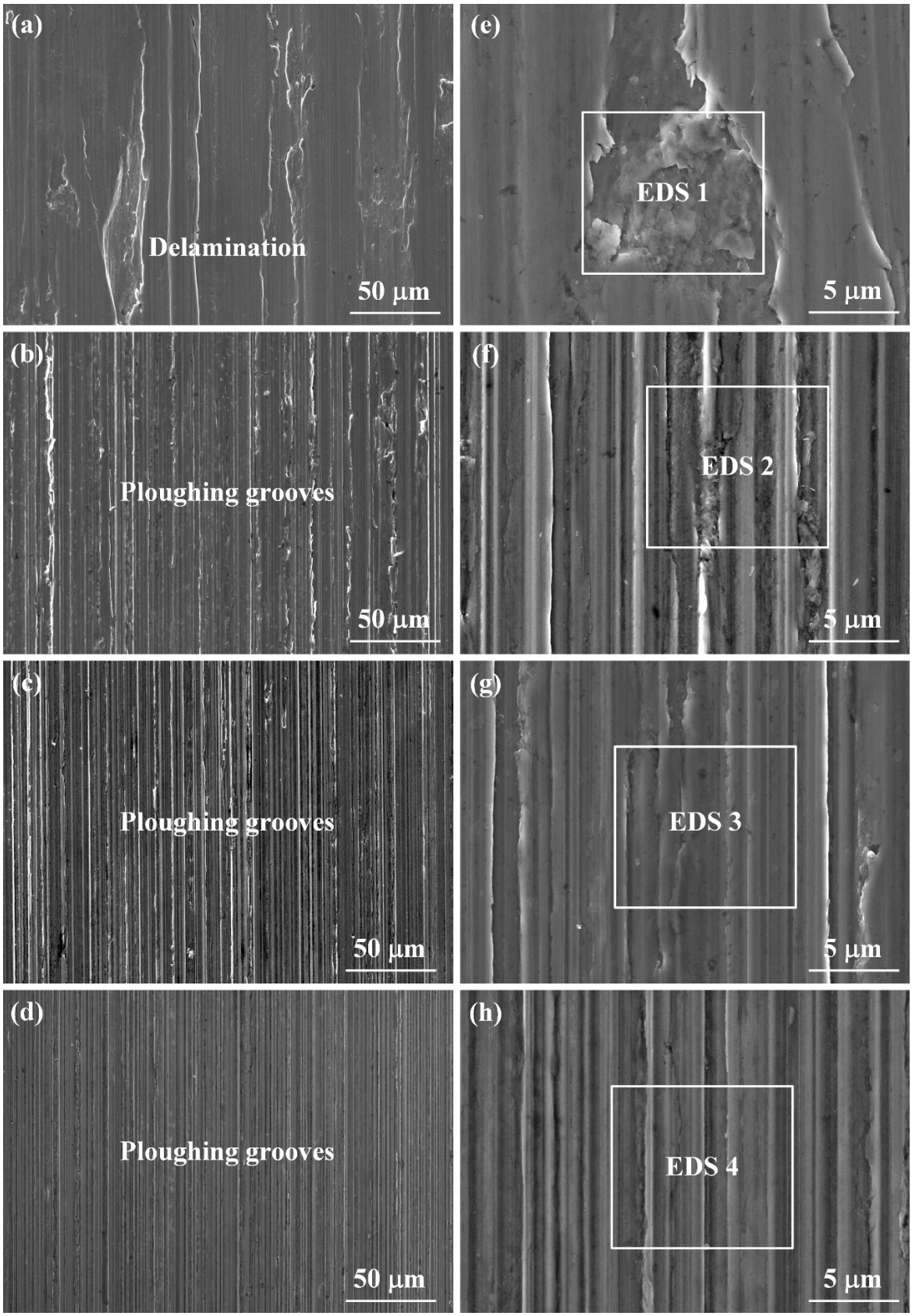

Figure 7. Worn surfaces generated using (**a**) water and (**b**) 0.06 wt.% ZrO_2, (**c**) 0.06 wt.% GO, and (**d**) 0.03–0.03 wt.% GO/ZrO_2 nanolubricants; (**e**–**h**) are their corresponding enlarged SEM images. Testing load = 20 N and sliding speed = 300 mm/s.

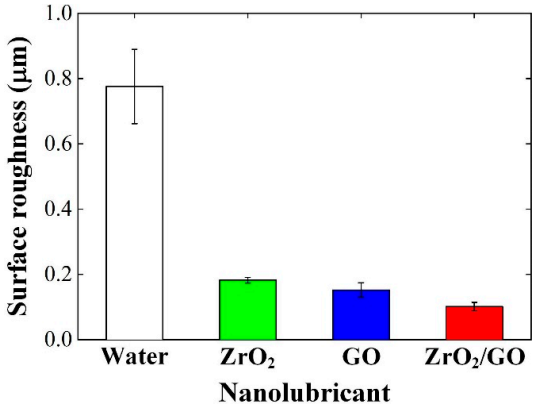

Figure 8. Averaged surface roughness (S_a) values achieved using water and 0.06 wt.% ZrO_2, 0.06 wt.% GO, and 0.03–0.03 wt.% ZrO_2/GO nanolubricants with an applied load of 20 N and a sliding speed of 300 mm/s.

3.5. Lubrication Mechanism Analysis

Understanding the roles of nanoadditives in water is crucial to optimizing the aqueous nanolubricant formulation for any specific mechanical contact system. To date, a number of lubrication mechanisms have been proposed to explain the improvement in lubrication with the application of nanoparticles as additives in water lubricants [7,28], including the ball bearing/rolling effect, polishing/smoothing effect, protective/lubricating film effect, and synergistic lubrication effect, as schematically illustrated in Figure 9. Nanoparticles with high hardness and spherical/rounded shapes can serve not only as tiny balls to generate a hybrid friction process of rolling and sliding to achieve decreased friction (see Figure 9a), but also polishing media to help smoothen surface asperities during sliding, thereby producing improved surface quality (see Figure 9b). Nanoparticles that possess moderate hardness and high chemical inertness likely form a protective film at the sliding area through a tribo-physical reaction, as displayed in Figure 9c. The film functions as a tribo-layer to lower friction and wear through improving asperity contact. Nanoadditives that have low hardness and lamellar structures, however, can deposit onto contact surfaces during sliding to generate a lubricating film through tribo-chemical or physical reactions, as shown in Figure 9d. The film can considerably lower friction and wear through relieving asperity ploughing. As illustrated in Figure 9e, hybrid nanoadditives consisting of two different dimensional nanomaterials can simultaneously obtain friction reduction and surface quality improvement through a synergistic lubrication effect produced by tribo-layer formation and asperity smoothing.

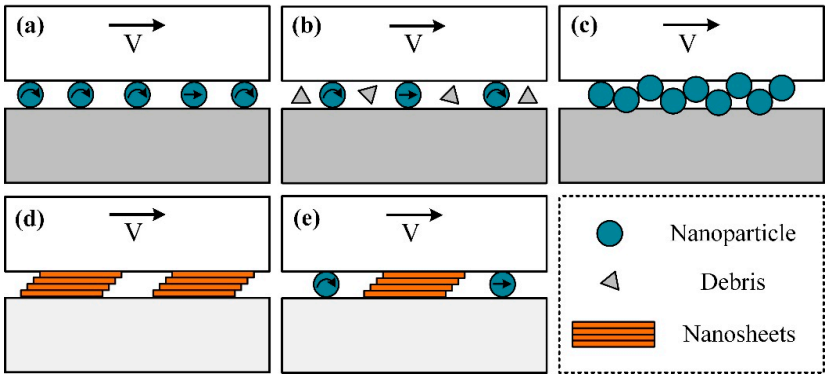

Figure 9. Lubrication mechanisms of nanoadditives suspended in water, including (**a**) rolling effect, (**b**) polishing effect, (**c**) protective film effect, (**d**) lubricating film effect, and (**e**) synergistic lubrication effect [7]. Reproduced with permission from [7]. Copyright Elsevier, 2022.

To understand the lubrication mechanism of ZrO_2, GO, and ZrO_2/GO nanolubricants, the corresponding worn surfaces were analysed using EDS and Raman microscopy. Figure 10a–d display the EDS spectra conducted on the squared areas marked on the worn block surfaces shown in Figure 7e–h, respectively, and the typical elements and their corresponding weight percentages are listed in Table 1. Zr was clearly detected on the worn surface lubricated with the ZrO_2 nanolubricant, as can be seen in Figure 10b, suggesting that during sliding the ZrO_2 nanoparticles dispersed in water formed a localised ZrO_2 tribo-layer on the rubbing areas [37]. This layer could help relieve asperity welding (i.e., adhesive wear), thus leading to the reduced friction force and the improved worn surface quality. Compared to water, higher C residue is observed on the worn surface of the GO nanolubricant, as displayed in Table 1. The corresponding Raman spectrum in Figure 10e shows two notable peaks at 1345 cm^{-1} and 1615 cm^{-1}, representing D and G bands of GO, respectively [34]. This result indicates that the GO nanosheets dispersed in water indeed participated in the sliding. The GO-related film could serve as a lubrication layer to improve asperity contact, leading to the reduced friction and wear. Similarly, the worn surface of the ZrO_2/GO nanolubricant detected a higher C content than that using water, but has no detectable signs of Zr on the rubbing area, as shown in Figure 10d. The corresponding Raman spectrum shown in Figure 10f exhibits no peaks of ZrO_2 in the range 200 to 800 cm^{-1} [38], while the spectrum obtained from the worn surface presents the typical D and G bands of GO. This was most likely because during sliding the ZrO_2 nanoparticles, instead of generating a deposit layer on the rubbing area, rolled between the contact surfaces with the lubricant flow due to the reduced interfacial shear resistance resulting from the GO nanosheets, as reported in [16]. In addition, as shown in Figure 10f, the intensity ratio of D to G bands (I_D/I_G) is 0.92, smaller than that of 1.04 on the worn surface lubricated with the GO nanolubricant. The decrease in I_D/I_G indicated lower defects on GO surfaces, which was ascribed to the improved lubrication as a result of the combination of ZrO_2 and GO [34]. The synergistic lubricating effect of GO nanosheets and the rolling effect of ZrO_2 nanoparticles helped suppress asperity welding and relieve asperity ploughing, thus resulting in the significantly improved tribological performance. In contrast, water alone could not prevent surface asperities from direct contact, thus resulting in the severe wear and friction.

Table 1. EDS analysis results of the squared areas marked on the worn surfaces shown in Figure 7e,f, generated using water, and the 0.06 wt.% ZrO_2, 0.06 wt.% GO, and 0.03–0.03 wt.% ZrO_2/GO nanolubricants.

Analysed Area	Lubricant	C	O	Zr	Cr	Ni	Mn	Si	Fe
EDS 1	Water	1.6	0.5	/	14.7	5.6	0.9	0.6	76.1
EDS 2	ZrO_2	1.8	1.7	0.9	17.0	7.3	1.2	0.4	69.7
EDS 3	GO	4.4	3.5	/	14.7	6.5	0.9	0.6	69.4
EDS 4	ZrO_2/GO	3.6	2.8	/	14.8	5.9	0.9	0.6	71.4

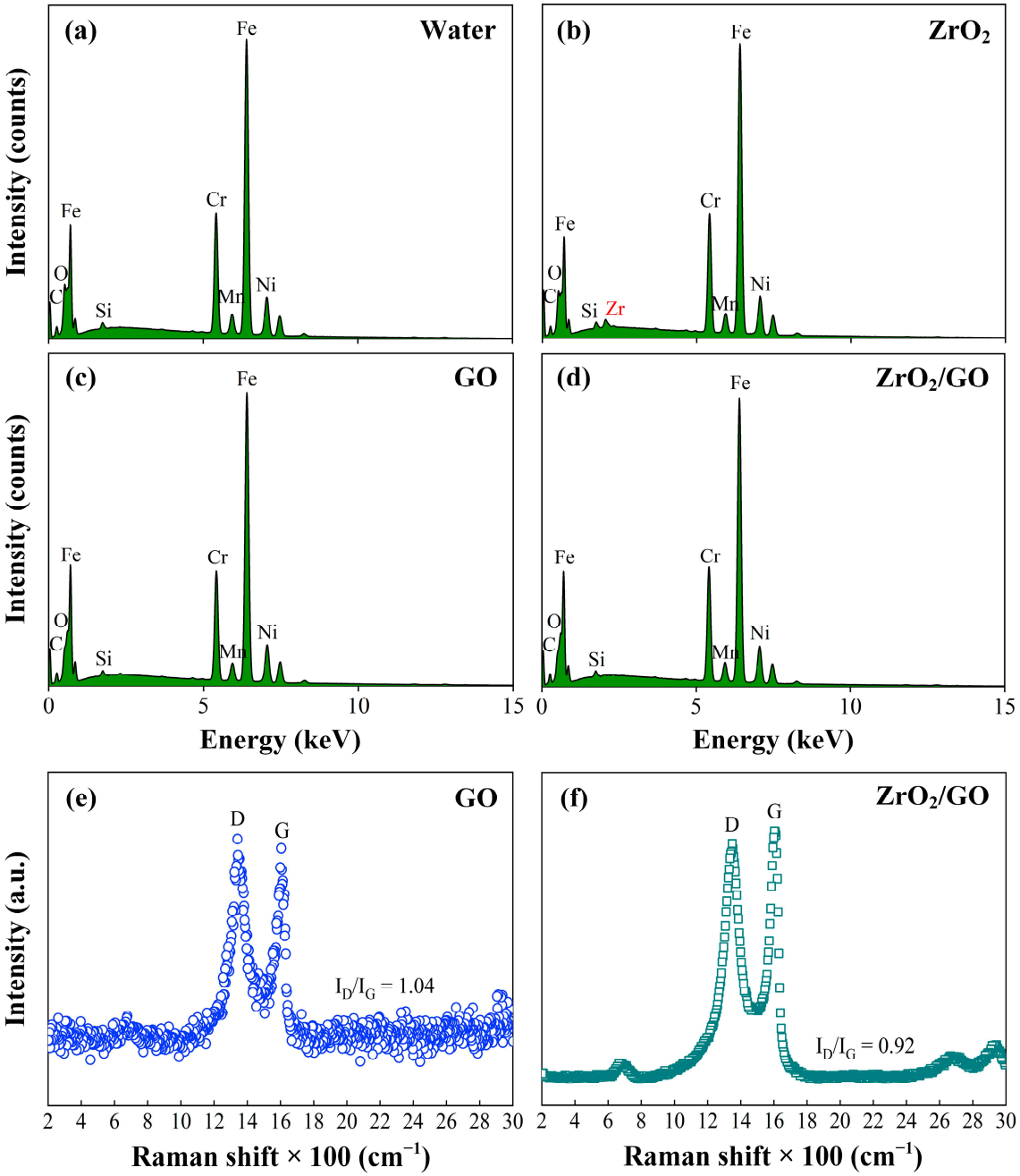

Figure 10. EDS spectra achieved with (**a**) water and (**b**) 0.06 wt.% ZrO_2, (**c**) 0.06 wt.% GO, and (**d**) 0.03–0.03 wt.% ZrO_2/GO nanolubricants, which were conducted on the squared areas marked in Figure 7e,f, respectively, and Raman spectra detected on the worn areas produced using (**e**) 0.06 wt.% GO and (**f**) 0.03–0.03 wt.% ZrO_2/GO nanolubricants.

4. Conclusions

Novel water-based hybrid nanolubricants were developed through ultrasonically dispersing ZrO_2 nanoparticles in GO aqueous suspensions, and their tribological performance was evaluated. The roles of nanoadditives in water-based nanolubrication were analysed and discussed. Key conclusions drawn from this study are shown below:

- Dimensional integration is an effective approach to improve nanoparticle dispersion in water.

- Addition of nanoadditives to water can improve its tribological performance, and there is an optimal concentration and mass ratio of nanoadditives for the best lubrication performance.
- In water-based lubrication, 0D-ZrO_2 nanoparticles are likely to generate a localised deposit layer on the rubbing area. This tribo-layer can help relieve asperity welding, i.e., adhesive wear, thus resulting in reduced friction and improved surface quality.
- In water-based lubrication, 2D-GO nanosheets tend to form a lubricating layer of low shear resistance on the sliding area. This self-lubricating layer can improve asperity contact and ploughing, thereby leading to reduced friction and wear.
- Hybrid nanoadditives of ZrO_2 nanoparticles and GO nanosheets can produce a synergistic friction-reduction and anti-wear effect in water-based lubrication, reliving abrasive wear (i.e., asperity ploughing) and suppressing adhesive wear (i.e., asperity welding), which thus enables the achievement of both improved tribological performance and enhanced surface quality.

Author Contributions: Conceptualization, S.H.; methodology, S.H.; validation, S.H.; formal analysis, S.H., Z.W., and L.X.; investigation, S.H; resources, S.H.; writing—original draft preparation, S.H.; writing—review and editing, S.H., Z.W., and L.X.; visualization, S.H.; supervision, C.H.; project administration, C.H.; funding acquisition, C.H. All authors have read and agreed to the published version of the manuscript.

Funding: This research was funded by the Baosteel-Australia Joint Research and Development Centre (BA17004), Australian Research Council (ARC) Industrial Transformation Research Hub for Computational Particle Technology (IH140100035), and Scientific Research Project for National High-level Innovative Talents of Hebei Province Full-time Introduction (2021HBQZYCXY004).

Institutional Review Board Statement: Not applicable.

Informed Consent Statement: Not applicable.

Data Availability Statement: The data presented in this study are available on request from the corresponding author.

Acknowledgments: S.H. would like to acknowledge the use of the facilities at, and the scientific and technical assistance of, the Nanomechanics and Advanced Manufacturing Laboratory at the University of Queensland.

Conflicts of Interest: The authors declare no conflict of interest.

References

1. Shokrani, A.; Dhokia, V.; Newman, S.T. Environmentally conscious machining of difficult-to-machine materials with regard to cutting fluids. *Int. J. Mach. Tool. Manu.* **2012**, *57*, 83–101. [CrossRef]
2. Zhang, Y.; Li, C.; Jia, D.; Zhang, D.; Zhang, X. Experimental evaluation of MoS_2 nanoparticles in jet MQL grinding with different types of vegetable oil as base oil. *J. Clean. Prod.* **2015**, *87*, 930–940. [CrossRef]
3. Reeves, C.J.; Siddaiah, A.; Menezes, P.L. Friction and wear behavior of environmentally friendly ionic liquids for sustainability of biolubricants. *J. Tribol.* **2019**, *141*, 051604. [CrossRef]
4. Siddaiah, A.; Kasar, A.K.; Manoj, A.; Menezes, P.L. Influence of environmental friendly multiphase lubricants on the friction and transfer layer formation during sliding against textured surfaces. *J. Clean. Prod.* **2019**, *209*, 1245–1251. [CrossRef]
5. Wu, H.; Jia, F.; Li, Z.; Lin, F.; Huo, M.; Huang, S.; Sayyar, S.; Jiao, S.; Huang, H.; Jiang, Z. Novel water-based nanolubricant with superior tribological performance in hot steel rolling. *Int. J. Extreme Manuf.* **2020**, *2*, 025002. [CrossRef]
6. Morshed, A.; Wu, H.; Jiang, Z. A comprehensive review of water-based nanolubricants. *Lubricants* **2021**, *9*, 89. [CrossRef]
7. Huang, S.; Wu, H.; Jiang, Z.; Huang, H. Water-based nanosuspensions: Formulation, tribological property, lubrication mechanism, and applications. *J. Manuf. Process.* **2021**, *71*, 625–644. [CrossRef]
8. Rahman, M.H.; Warneke, H.; Webbert, H.; Rodriguez, J.; Austin, E.; Tokunaga, K.; Rajak, D.K.; Menezes, P.L. Water-based lubricants: Development, properties, and performances. *Lubricants* **2021**, *9*, 73. [CrossRef]
9. Wu, H.; Kamali, H.; Huo, M.; Lin, F.; Huang, S.; Huang, H.; Jiao, S.; Xing, Z.; Jiang, Z. Eco-friendly water-based nanolubricants for industrial-scale hot steel rolling. *Lubricants* **2020**, *8*, 96. [CrossRef]
10. Sun, J.; Meng, Y.; Zhang, B. Tribological behaviors and lubrication mechanism of water-based MoO_3 nanofluid during cold rolling process. *J. Manuf. Process.* **2021**, *61*, 518–526. [CrossRef]
11. Meng, Y.; Sun, J.; He, J.; Yan, X.; Pei, Y. Recycling prospect and sustainable lubrication mechanism of water-based MoS_2 nano-lubricant for steel cold rolling process. *J. Clean. Prod.* **2020**, *277*, 123991.

12. Musavi, S.H.; Davoodi, B.; Niknam, S.A. Effects of reinforced nanoparticles with surfactant on surface quality and chip formation morphology in MQL-turning of superalloys. *J. Manuf. Process.* **2019**, *40*, 128–139. [CrossRef]
13. Wu, H.; Jia, F.; Zhao, J.; Huang, S.; Wang, L.; Jiao, S.; Huang, H.; Jiang, Z. Effect of water-based nanolubricant containing nano-TiO_2 on friction and wear behaviour of chrome steel at ambient and elevated temperatures. *Wear* **2019**, *426*, 792–804. [CrossRef]
14. Wu, H.; Zhao, J.; Luo, L.; Huang, S.; Wang, L.; Zhang, S.; Jiao, S.; Huang, H.; Jiang, Z. Performance evaluation and lubrication mechanism of water-based nanolubricants containing nano-TiO_2 in hot steel rolling. *Lubricants* **2018**, *6*, 57. [CrossRef]
15. He, A.; Huang, S.; Yun, J.-H.; Wu, H.; Jiang, Z.; Stokes, J.; Jiao, S.; Wang, L.; Huang, H. Tribological performance and lubrication mechanism of alumina nanoparticle water-based suspensions in ball-on-three-plate testing. *Tribol. Lett.* **2017**, *65*, 40. [CrossRef]
16. Huang, S.; Lin, W.; Li, X.; Fan, Z.; Wu, H.; Jiang, Z.; Huang, H. Roughness-dependent tribological characteristics of water-based GO suspensions with ZrO_2 and TiO_2 nanoparticles as additives. *Tribol. Int.* **2021**, *161*, 107073. [CrossRef]
17. He, A.; Huang, S.; Yun, J.-H.; Jiang, Z.; Stokes, J.R.; Jiao, S.; Wang, L.; Huang, H. Tribological characteristics of aqueous graphene oxide, graphitic carbon nitride, and their mixed suspensions. *Tribol. Lett.* **2018**, *66*, 42. [CrossRef]
18. Kinoshita, H.; Nishina, Y.; Alias, A.A.; Fujii, M. Tribological properties of monolayer graphene oxide sheets as water-based lubricant additives. *Carbon* **2014**, *66*, 720–723. [CrossRef]
19. Song, H.J.; Na, L. Frictional behavior of oxide graphene nanosheets as water-base lubricant additive. *Appl. Phys. A* **2011**, *105*, 827–832. [CrossRef]
20. Hu, Y.; Wang, Y.; Zeng, Z.; Zhao, H.; Ge, X.; Wang, K.; Wang, L.; Xue, Q. PEGlated graphene as nanoadditive for enhancing the tribological properties of water-based lubricants. *Carbon* **2018**, *137*, 41–48. [CrossRef]
21. Peña-Parás, L.; Maldonado-Cortés, D.; Rodríguez-Villalobos, M.; Romero-Cantú, A.G.; Montemayor, O.E. Enhancing tool life, and reducing power consumption and surface roughness in milling processes by nanolubricants and laser surface texturing. *J. Clean. Prod.* **2020**, *253*, 119836. [CrossRef]
22. Peña-Parás, L.; Maldonado-Cortés, D.; Rodríguez-Villalobos, M.; Romero-Cantú, A.G.; Montemayor, O.E.; Herrera, M.; Trousselle, G.; González, J.; Hugler, W. Optimization of milling parameters of 1018 steel and nanoparticle additive concentration in cutting fluids for enhancing multi-response characteristics. *Wear* **2019**, *426–427*, 877–886. [CrossRef]
23. Lin, C.-L.; Lin, W.; Huang, S.; Edwards, G.; Lu, M.; Huang, H. Tribological performance of zeolite/sodium dodecylbenzenesulfonate hybrid water-based lubricants. *Appl. Surf. Sci.* **2022**, *598*, 153764. [CrossRef]
24. Li, X.; Huang, S.; Wu, Y.; Huang, H. Performance evaluation of graphene oxide nanosheet water coolants in the grinding of semiconductor substrates. *Precis. Eng.* **2019**, *60*, 291–298. [CrossRef]
25. Li, C.; Li, X.; Huang, S.; Li, L.; Zhang, F. Ultra-precision grinding of $Gd_3Ga_5O_{12}$ crystals with graphene oxide coolant: Material deformation mechanism and performance evaluation. *J. Manuf. Process.* **2021**, *61*, 417–427. [CrossRef]
26. Huang, H.; Li, X.; Mu, D.; Lawn, B.R. Science and art of ductile grinding of brittle solids. *Int. J. Mach. Tool. Manu.* **2021**, *161*, 103675. [CrossRef]
27. Wu, Y.; Mu, D.; Huang, H. Deformation and removal of semiconductor and laser single crystals at extremely small scales. *Int. J. Extreme Manuf.* **2020**, *2*, 012006. [CrossRef]
28. Wu, H.; Zhao, J.; Xia, W.; Cheng, X.; He, A.; Yun, J.H.; Wang, L.; Huang, H.; Jiao, S.; Huang, L. A study of the tribological behaviour of TiO2 nano-additive water-based lubricants. *Tribol. Int.* **2017**, *109*, 398–408. [CrossRef]
29. Yang, J.; Xia, Y.; Song, H.; Chen, B.; Zhang, Z. Synthesis of the liquid-like graphene with excellent tribological properties. *Tribol. Int.* **2017**, *105*, 118–124. [CrossRef]
30. He, A.; Huang, S.; Yun, J.-H.; Jiang, Z.; Stokes, J.; Jiao, S.; Wang, L.; Huang, H. The pH-dependent structural and tribological behaviour of aqueous graphene oxide suspensions. *Tribol. Int.* **2017**, *116*, 460–469. [CrossRef]
31. Wu, H.; Zhao, J.; Xia, W.; Cheng, X.; He, A.; Yun, J.H.; Wang, L.; Huang, H.; Jiao, S.; Huang, L. Analysis of TiO_2 nano-additive water-based lubricants in hot rolling of microalloyed steel. *J. Manuf. Process.* **2017**, *27*, 26–36. [CrossRef]
32. Das, A.; Pradhan, O.; Patel, S.K.; Das, S.R.; Biswal, B.B. Performance appraisal of various nanofluids during hard machining of AISI 4340 steel. *J. Manuf. Process.* **2019**, *46*, 248–270. [CrossRef]
33. Peña-Parás, L.; Rodríguez-Villalobos, M.; Maldonado-Cortés, D.; Guajardo, M.; Rico-Medina, C.S.; Elizondo, G.; Quintanilla, D.I. Study of hybrid nanofluids of TiO_2 and montmorillonite clay nanoparticles for milling of AISI 4340 steel. *Wear* **2021**, *477*, 203805. [CrossRef]
34. Huang, S.; He, A.; Yun, J.-H.; Xu, X.; Jiang, Z.; Jiao, S.; Huang, H. Synergistic tribological performance of a water based lubricant using graphene oxide and alumina hybrid nanoparticles as additives. *Tribol. Int.* **2019**, *135*, 170–180. [CrossRef]
35. He, J.; Sun, J.; Meng, Y.; Pei, Y. Superior lubrication performance of MoS_2-Al_2O_3 composite nanofluid in strips hot rolling. *J. Manuf. Process.* **2020**, *57*, 312–323. [CrossRef]
36. Liu, Y.; Wang, X.; Pan, G.; Luo, J. A comparative study between graphene oxide and diamond nanoparticles as water-based lubricating additives. *Sci. China Technol. Sci.* **2013**, *56*, 152–157. [CrossRef]
37. Wu, H.; Zhao, J.; Cheng, X.; Xia, W.; He, A.; Yun, J.-H.; Huang, S.; Wang, L.; Huang, H.; Jiao, S. Friction and wear characteristics of TiO_2 nano-additive water-based lubricant on ferritic stainless steel. *Tribol. Int.* **2018**, *117*, 24–38. [CrossRef]
38. Ji, P.; Mao, Z.; Wang, Z.; Xue, X.; Zhang, Y.; Lv, J.; Shi, X. Improved surface-enhanced raman scattering properties of ZrO_2 Nanoparticles by Zn Doping. *Nanomaterials* **2019**, *9*, 983. [CrossRef]